

# Discrete-dipole approximation on a rectangular cuboidal point lattice: considering dynamic depolarization

Enrico Massa,\* Tyler Roschuk, Stefan A. Maier, and Vincenzo Giannini

*Blackett Laboratory, Department of Physics, Imperial College London, London SW7 2AZ, UK*

*\*Corresponding author: enrico.massa08@imperial.ac.uk*

Received October 22, 2013; revised November 25, 2013; accepted November 27, 2013;  
posted December 2, 2013 (Doc. ID 199735); published December 16, 2013

Discrete-dipole approximation (DDA), which is used for computing scattering and absorption by particles of arbitrary geometry and material, is extended to the case of a rectangular cuboidal point lattice using an accurate, analytical expression of the polarizability of each cuboidal element at optical frequencies of up to 100 nm in size. This polarizability formulation (cuboidal lattice with depolarization or CLD) is shown to be more accurate in the computation of the extinction, scattering, and absorption cross sections when simulating dielectrics compared to other available and commonly used expressions of the polarizability. This can be used to reduce the number of dipoles  $N$  used, and therefore, the computation time while achieving the same accuracy of other formulations. The CLD formulation was applied to the Mie scattering problem and the results were compared to results from other DDA formulations, as well as to the Mie analytical solution for metal and dielectric spheres. Metal cubes were also simulated and different formulations compared. © 2013 Optical Society of America

*OCIS codes:* (290.5825) Scattering theory; (240.6680) Surface plasmons; (050.1755) Computational electromagnetic methods; (260.2110) Electromagnetic optics.

<http://dx.doi.org/10.1364/JOSAA.31.000135>

## 1. INTRODUCTION

Discrete-dipole approximation (DDA) [1–4] is a powerful technique used for computing the scattering and absorption by particles of arbitrary geometry and material. The DDA technique has been used for many difficult scattering problems. Thanks to the development of efficient algorithms and the availability of inexpensive computing power, the DDA technique has been studied extensively and numerous advances have been achieved, such as the use of the complex-conjugate gradient (CCG) and the fast-Fourier-transform (FFT) to permit the solution of problems involving large values of  $N$  representing the number of point dipoles [1,5,6]. Indeed, the computational complexity of the method scales, depending on the method used, as  $O(N^3)$  using direct inversion, as  $O(N_{\text{iter}}N^2)$  using iterative solvers such as the CCG, or as  $O(N_{\text{iter}}N \log N)$  using iterative solvers together with the FFT technique, where  $N_{\text{iter}}$  is the number of iterations of the solver. Usually, a high number of dipoles,  $N$ , is needed to achieve convergence, so the use of iterative solvers can speed up the computations significantly when  $N_{\text{iter}} \ll N$ . However, in general, iterative methods converge in  $O(N)$  iterations and convergence is not guaranteed, although in most cases convergence to the required level of accuracy is obtained for  $N_{\text{iter}} \ll N$  [7]. It is, therefore, of great interest to develop a method for reducing the number of dipoles needed in the computation while obtaining similar accuracy; this would give a very significant speed up to the calculations. This paper extends the DDA technique to use a general cuboidal point lattice by employing a formula for the polarizability of the cuboidal dipole element that takes into account the depolarization, which is accurate up to 100 nm in size at optical frequencies. In this work, the formulation of the polarizability for the DDA will be called the “cuboidal lattice with depolarization” or, in short, CLD.

Several different formulations of the polarization for the DDA for a cubic lattice have been proposed in the past, in order to describe the polarization of each cubic element. The most commonly used formulations are the lattice dispersion relation (LDR) [8], filtered coupled dipoles (FCD) [9], integration of Green’s tensor (IGT), which is analytical to the second-order (IGTSO) [10,11], and Clausius–Mossotti with radiative corrections (RRC). In the case of a cubical lattice, the CLD gives the same result as the IGTSO formulation, so it can be considered an extension of the IGTSO to nonequidimensional lattices. As we shall see, the CLD polarizability formulation is more accurate in the computation of the extinction, scattering, and absorption cross sections when simulating dielectrics, compared to other available and commonly used expressions of the polarizability. This increase in accuracy is only due to an improved formulation of the polarizability, since in all cases the interaction term is taken to be dipole–dipole. The improved accuracy can be used to reduce the number of dipoles  $N$  used, and therefore, the computation time while achieving the same accuracy of other formulations. Additionally, the CLD formulation works as well as the other formulations in the case of metals. In particular, we will show that the formulation works well when localized surface plasmons are excited, which makes it possible to study the plasmon resonance of metal nanoparticles [7,12–14] in many promising applications such as enhancing light emission [13,15] and in THz plasmonics [16]. This work aims to provide a prescription for the dipole polarizability for a cuboidal point lattice that supersedes other formulations of the polarizability, which are available only for cubical lattices. This allows one to have lattices with unit cells of different sizes and aspect ratios and enables a more accurate discretization of specific geometries, e.g., curved shapes and the treatment of problems

with large field variations (using lattice refinement). In this paper, in order to compare our results to those from other available formulations of the polarizability, we will restrict our calculations to cubical lattices. This is the first DDA formulation that uses an analytical expression for the polarizability of a rectangular cuboidal point lattice because, previously, similar calculations were done by numerical integration of the Green's tensor to express the polarizability [10,17], which is computationally more expensive.

## 2. DISCRETE-DIPOLE APPROXIMATION (DDA)

Our aim is to calculate the scattering and absorption properties of an object of arbitrary geometry. Exact solutions of the scattering problem from Maxwell's equations are available only for special geometries such as spheres, spheroids [18,19], and infinite cylinders. Numerical methods such as the DDA are required for other geometries. The DDA aims to approximate a continuum object by a finite array of polarizable points. The polarizable points acquire a dipole moment in response to the local electric field, while the dipoles interact with one another via their electric field. The theoretical base for DDA, which was first introduced by Purcell and Pennypacker [2], is summarized by Draine and Flatau [1,3]. A more general and rigorous theory based on the Green's function formulation is summarized by Yurkin and Hoekstra [4]. Given that the dielectric properties of a substance can be directly related to the polarizabilities of the individual atoms of which it is composed, and that the continuum representation of a solid is appropriate on length scales that are large compared to the interparticle spacing, we may expect that an array of polarizable points can accurately approximate the response of a continuum object on length scales that are large compared to the interdipole separation. In the case of a finite array of point dipoles, the scattering problem can be solved exactly so that the unique approximation of the DDA is the replacement of the continuum object by an array of  $N$ -point dipoles. It is worth noting that the DDA result converges to the exact value with refining discretizations, therefore, it is a rigorous method to solve Maxwell's equations [20]. The solution to the problem requires specifying both the geometry, that is the location of the dipoles ( $\mathbf{r}_j, j = 1, \dots, N$ ), and the point dipole polarizabilities  $\alpha_j$ . In the case of a monochromatic incident wave, a self-consistent solution for the polarization  $\mathbf{P}_j$  can be found and from these  $\mathbf{P}_j$  values the absorption and scattering cross sections are obtained. The DDA can be readily applied to anisotropic materials given that the point dipole polarizabilities may be tensors. Moreover, the DDA can treat materials with nonzero magnetic susceptibility, such as bianisotropic materials [21], and can be used to calculate magneto-optical spectra [22].

### A. PROBLEM OF POLARIZABILITY

In the DDA, each dipole represents the dipole moment of a particular subvolume of the scattering object. In order to approximate the target geometry (e.g., a sphere, a cube, etc.) with a finite number of dipoles, one may generate several meshes that are defined by the coordinates of each of the lattice points. The aim here is to best capture the geometry in such a way that the number of points in the dipole array is not so large as to be computationally prohibitive. Given the

list of sites  $j = 1, \dots, N$ , we considered that each of the sites represents a subvolume of material respectively centered on the site with its corresponding volume  $V_j$ , and we assigned it a dipole polarizability,  $\alpha_j$ , which can be a tensor in the most general case. The DDA can be thought of as a scattering problem, i.e., finding the values of the polarization  $\mathbf{P}_j$  for the target array of point dipoles ( $j = 1, \dots, N$ ) with polarizabilities  $\alpha_j$ , located at the positions  $\mathbf{r}_j$ , with  $\mathbf{E}_j$  being the electric field at  $\mathbf{r}_j$  due to the incident field  $\mathbf{E}_{\text{inc},j} = \mathbf{E}_0 \exp(i\mathbf{k}_B \cdot \mathbf{r}_j - i\omega t)$ , where  $k_B = \omega/c\sqrt{\epsilon_B}$  and  $\epsilon_B$  is the background dielectric constant, plus the contribution of the scattered field from the other  $N - 1$  surrounding dipoles, following the approach summarized by Draine and Flatau [1,3].

The same problem can be treated in the more general framework of Green's function [4,23], which has the advantage of making all the assumptions more clear. From the definition of Green's tensor and introducing the discretized field  $\mathbf{E}_i = \mathbf{E}(\mathbf{r}_i)$ , the discretized Green's tensor  $\mathbf{G}_{i,j}^B = \mathbf{G}^B(\mathbf{r}_i, \mathbf{r}_j)$  and the discretized dielectric contrast  $\Delta\epsilon_i = \epsilon(\mathbf{r}_i) - \epsilon_B$ , the electric field inside the scatterer can be written as a system of linear equations:

$$\mathbf{E}_i = \mathbf{E}_{\text{inc},i} + \sum_{j=1, j \neq i}^N \mathbf{G}_{i,j}^B \cdot \frac{\Delta\epsilon_j}{\epsilon_B} \mathbf{E}_j V_j + \mathbf{M}_i \cdot \frac{\Delta\epsilon_i}{\epsilon_B} \mathbf{E}_i - \mathbf{L} \cdot \frac{\Delta\epsilon_i}{\epsilon_B} \mathbf{E}_i, \quad i = 1, \dots, N, \quad (1)$$

with the self term  $\mathbf{M}_i$  defined as:

$$\mathbf{M}_i = \lim_{\delta V \rightarrow 0} \int_{V_i - \delta V} \mathbf{dr}' G^B(\mathbf{r}_i, \mathbf{r}'), \quad (2)$$

and with the source dyadic  $\mathbf{L}$ , which depends on the shape of the exclusion volume  $\delta V$  used to eliminate the singularity of the integrand, as derived in detail by Yaghjian [24]. By defining the polarizability tensor as:

$$\alpha_i = V_i \frac{\Delta\epsilon}{\epsilon_B} \left( \mathbf{I} + (\mathbf{L}_i - \mathbf{M}_i) \frac{\Delta\epsilon}{\epsilon_B} \right)^{-1}, \quad (3)$$

it is possible to formulate the DDA problem as:

$$\mathbf{E}_{\text{inc},i} = \alpha_i^{-1} \mathbf{P}_i - \sum_{j=1, j \neq i}^N \mathbf{G}_{i,j} \mathbf{P}_j, \quad i = 1, \dots, N, \quad (4)$$

where the Green's tensor has the explicit form of:

$$\mathbf{G}^B(\mathbf{r}_i, \mathbf{r}_j) = \left[ k_B \left( \mathbf{I} - \frac{\mathbf{R}\mathbf{R}}{R^2} \right) - \frac{1 - ik_B R}{R^2} \left( \mathbf{I} - 3 \frac{\mathbf{R}\mathbf{R}}{R^2} \right) \right] \frac{\exp(ik_B R)}{4\pi R}, \quad (5)$$

with  $R = |\mathbf{R}| = |\mathbf{r}_i - \mathbf{r}_j|$ , and we have used the definition of the polarization:

$$\mathbf{P}_i = \frac{\Delta\epsilon_i}{\epsilon_B} V_i \mathbf{E}_i. \quad (6)$$

Clearly, choosing different types of cells with the same volume yields a different value of the polarizability  $\alpha$ . For a cubical cell, neglecting the self term  $\mathbf{M}_i$ , the well-known Clausius–Mossotti (CM) polarizability is obtained:

$$\alpha_i^{\text{CM}} = 3d^3 \frac{\epsilon_i - \epsilon_B}{\epsilon_i + 2\epsilon_B}, \quad (7)$$

where  $d$  is the size of the cubical cell. In this form, the CM polarizability does not satisfy energy conservation, therefore, in order to satisfy the optical theorem, the radiative reaction correction (RRC) is normally added to obtain [25]:

$$\alpha_i^{\text{RRC}} = \frac{\alpha_i^{\text{CM}}}{1 - \frac{1}{6\pi} ik_B^3 \alpha_i^{\text{CM}}}. \quad (8)$$

There are many other types of prescriptions for the polarizability that can be used in the DDA to describe a cubical lattice, and they can be normally reduced to the CM + RRC with higher order corrections. One of the most commonly used is the LDR introduced by Draine and Goodman [8], which was determined as the polarizability for which plane waves propagate in the same way as in a medium with a given refractive index in an infinite lattice of point dipoles. Another is the FCD [9], where the Green's function and the susceptibility are sampled using an antialiasing filter in order to obtain an analytical expression of the self term  $M_i$ . In the integration of Green's tensor (IGT) technique [10], a Weyl expansion of the Green's tensor is performed in order to evaluate numerically the term  $L - M$ . All these formulations of the polarizability with the self term  $M_i \neq 0$  differ in the way they take into account the effect of the depolarization on each cell element due to the matter surrounding the center of the cell. This effect is of considerable importance to achieve good convergence for relatively larger values of the spacing between dipoles, i.e., for a smaller number of dipoles  $N$ , however, it tends to zero for  $N \rightarrow \infty$  ( $V_j \rightarrow 0$ ). Therefore, all formulations of the polarizability for a value of  $N$  high enough are equivalent since they converge to the same result, but practically, for the computation, using a good approximation of the polarizability is very important. However, these formulations (except for the IGT for which a numerical integration on a cuboid is possible) are applicable just for a cubical lattice and not for a more general cuboidal lattice, which may be more suitable for modeling some situations such as objects with different aspect ratios.

In this paper, we propose a prescription of the polarizability that considers the depolarization valid for a general cuboidal lattice, which was calculated analytically by integration of the Green's function expansion on a cuboidal element [26]. For a cube, this formulation gives the same result as the IGT formulation to the second-order (IGTSO) [11]. The polarizability of a cuboidal subvolume of length  $L_a = 2a$ , width  $L_b = 2b$ , and height  $L_c = 2c$ , for incident light polarized along the length, is:

$$\alpha = \frac{8abc}{\frac{\epsilon_B}{\epsilon - \epsilon_B} - \frac{1}{4\pi} \left[ -2\Omega + \frac{k_B^2}{2} \beta + \frac{16}{3} ik_B^3 abc \right]}, \quad (9)$$

where  $\Omega$  is defined as:

$$\Omega = 4 \arcsin \left( \frac{bc}{\sqrt{(a^2 + b^2)(a^2 + c^2)}} \right), \quad (10)$$

and  $\beta$  is the dynamic geometrical depolarization factor, defined as:

$$\beta = \int_{-c}^c \int_{-b}^b \int_{-a}^a \frac{1}{\sqrt{x^2 + y^2 + z^2}} \left( 1 + \frac{x^2}{x^2 + y^2 + z^2} \right) dx dy dz, \quad (11)$$

which has an analytical expression [26]. For a cube, it is expressed by:

$$\beta_{\text{cube}} = 16 \left[ \log \left( \frac{\sqrt{3} + 1}{\sqrt{3} - 1} \right) - \frac{\pi}{6} \right] a^2 \approx 12.6937a^2. \quad (12)$$

The polarizability for incident light polarized along the other directions (i.e., along the width and height) can be obtained from Eq. (9) by a simple permutation of the labels  $a$ ,  $b$ , and  $c$  for the length, width, and height, respectively. These expressions have been shown to predict well the polarizability of cuboids up to 100 nm in size, but for our DDA calculations we will consider a smaller discretization [26]. There are two obvious criteria on the discretization spacing for the validity of the DDA: the first is that the lattice spacing between the dipoles is small compared to the incident wavelength in the target material and the second is that the lattice spacing is small enough to describe the shape of the object satisfactorily.

From the polarizations  $P_j$ , calculated by solving Eq. (4), the extinction, scattering, and absorption cross sections can be obtained. The extinction cross section is calculated using:

$$\sigma_{\text{ext}} = \frac{k_B}{|E_0|^2} \sum_{j=1}^N \Im(\bar{E}_{\text{inc},j} \cdot P_j). \quad (13)$$

The absorption cross section can be obtained by summing the rate of energy dissipation by each of the dipoles, and by including the radiative correction, it can be shown to be:

$$\sigma_{\text{abs}} = \frac{k_B}{|E_0|^2} \sum_{j=1}^N \left\{ \Im(\bar{E}_j \cdot P_j) - \frac{1}{6\pi} k_B^3 \bar{P}_j \cdot P_j \right\}, \quad (14)$$

where  $\bar{z}$  is the complex conjugate of  $z$ . The scattering cross section can then be obtained as the difference between the extinction and the absorption cross sections, but when the absorption is dominant, it requires both of the cross sections to be calculated to high accuracy [1].

### 3. RESULTS AND DISCUSSION

For all our calculations we used a modified version of ADDA [11,27], which implements the CLD polarizability. The results obtained with the CLD polarizability were the same as the ones using the IGTSO implemented in ADDA. This is understandable since both methods are based on the integration of the Green's function on a lattice element. The advantage of the CLD is to provide an analytical expression valid for a general cuboidal lattice in order to avoid a numerical integration as in the IGT. To validate our results we compared the DDA results using the CLD polarizability for a cubic lattice with the other available prescriptions for the polarizability, in particular the RRC, FCD, and LDR. We also compared the results with Mie theory when simulating spheres. For our comparisons, we considered the case of gold (Au) and dielectric (refractive index  $m = 2$ ) nanoantennas in a vacuum ( $\epsilon_B = 1$ ). The dielectric function of Au was expressed using the Drude model,

which fits well to the experimental dielectric function but neglects the interband transition region. Note that this is chosen only for convenience during the comparison. In fact, the DDA works with an arbitrary dielectric function  $\epsilon$ , and therefore, also with any experimental dielectric function. In particular, we have simulated gold using the following expression:

$$\epsilon(\omega) = \epsilon_\infty - \frac{\omega_p^2}{\omega(\omega + i\gamma)}, \quad (15)$$

where  $\epsilon_\infty = 10.7026$ ,  $\omega_p$  is the plasma frequency ( $\omega_p = 1.3748 \cdot 10^{16}$  Hz), and  $\gamma$  is the collision frequency ( $\gamma = 1.1738 \cdot 10^{14}$  Hz).

Figure 1 shows the comparison of the extinction cross section for gold and dielectric spheres of different sizes using the DDA with CLD polarizability and Mie theory with a fixed number of dipoles per lambda (Dpl = 100). The agreement is very good, and, as expected, is better for dielectrics because of the inherent limitations of the DDA. In all cases the spectra show a well defined localized surface plasmon resonance. In Fig. 2, we compared the relative error ( $|\sigma - \sigma_{\text{Mie}}|/\sigma_{\text{Mie}}$ ) in the extinction cross section for gold and dielectric spheres of radius  $R = 150$  nm for different prescriptions of the polarizability (RRC, CLD, FCD, and LDR), while changing the number of dipoles per lambda (Dpl). This rigorous comparison is possible thanks to the exact values of the cross sections provided by Mie theory. The relative error was averaged across the entire range of wavelengths, i.e., from 300 to 800 nm. The relative

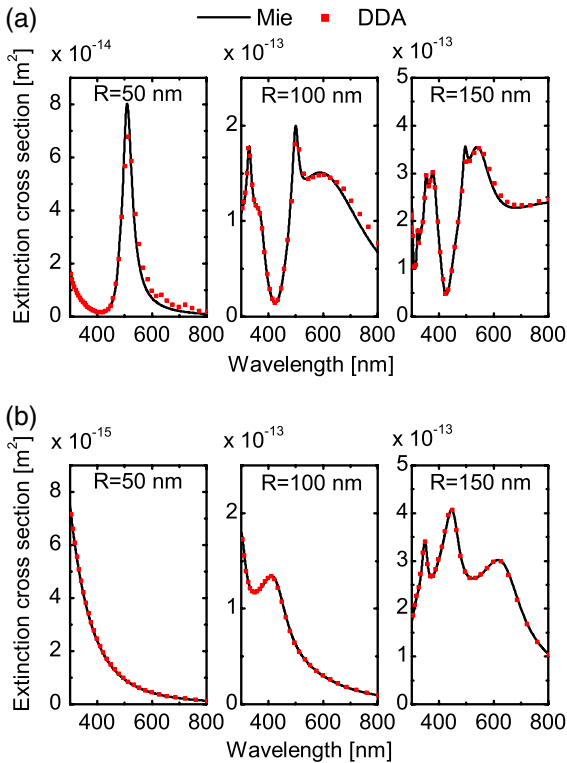


Fig. 1. Comparison between the extinction cross sections, calculated using Mie theory and the DDA with CLD polarizability, of (a) gold (Au) and (b) dielectric (refractive index  $m = 2$ ) spheres of radii  $R = 50$ , 100, and 150 nm placed in a vacuum ( $\epsilon_B = 1$ ). The DDA calculations were done with a fixed number of dipoles per lambda (Dpl = 100). The spectra for gold spheres show a well defined localized plasmon resonance.

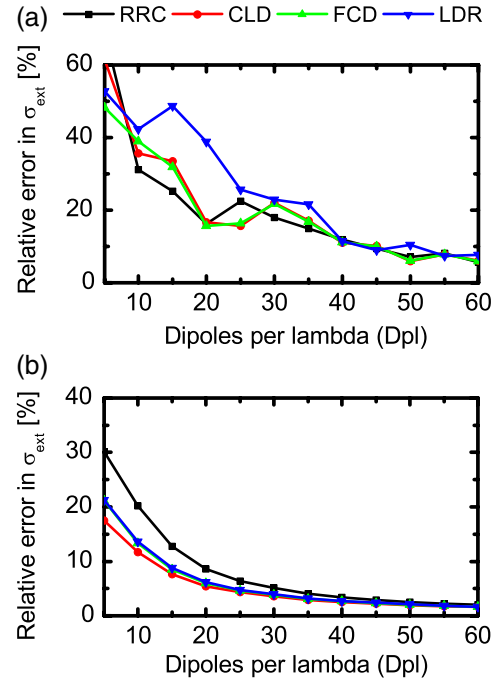


Fig. 2. Comparison of the averaged relative error (compared to Mie theory) in the extinction cross section ( $\sigma_{\text{ext}}$ ) for (a) a gold and (b) dielectric (refractive index  $m = 2$ ) sphere of radius  $R = 150$  nm for different prescriptions of the polarizability with a changing number of dipoles per lambda (Dpl). The relative error was averaged across the entire range of wavelengths, i.e., from 300 to 800 nm. For dielectrics, the CLD prescription had the lowest relative error, followed by FCD and LDR, with the RRC last. For metals, all prescriptions showed similar behavior.

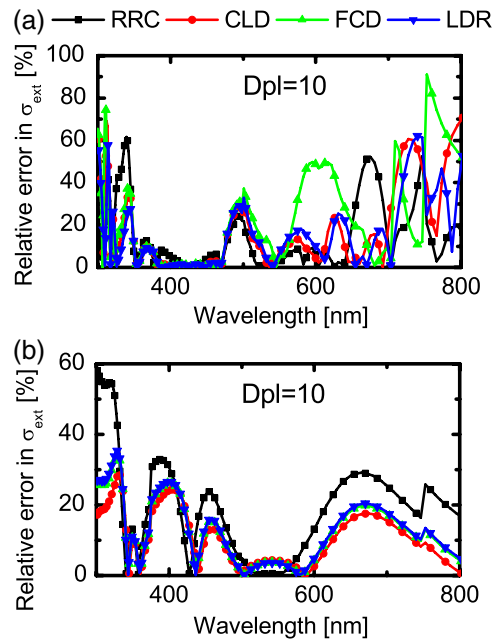


Fig. 3. Comparison of the relative error (compared to Mie theory) in the extinction cross section ( $\sigma_{\text{ext}}$ ) for (a) a gold and (b) dielectric (refractive index  $m = 2$ ) sphere of radius  $R = 150$  nm for different prescriptions of the polarizability with a fixed low number of dipoles per lambda (Dpl = 10). For dielectrics, the CLD prescription had the lowest relative error, followed by FCD and LDR, with the RRC last. For metals, all prescriptions showed similar behavior.

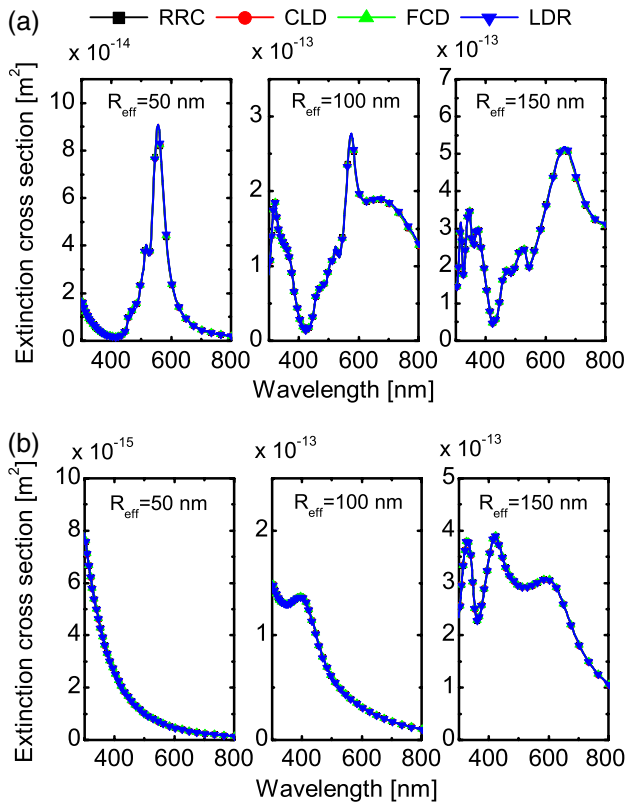


Fig. 4. Comparison between the extinction cross sections, calculated using the DDA with different prescriptions for the polarizability, of (a) gold (Au) and (b) dielectric (refractive index  $m = 2$ ) cubes of effective radii  $R_{\text{eff}} = 50, 100,$  and  $150$  nm placed in a vacuum ( $\epsilon_B = 1$ ). The DDA calculations were done with a fixed number of dipoles per lambda ( $D_{\text{pl}} = 100$ ). The spectra for gold cubes show a well defined localized plasmon resonance. The smaller peaks arose because of higher order modes than the main dipolar peak [29].

errors at each wavelength are shown in Fig. 3 for a fixed number of dipoles per lambda ( $D_{\text{pl}} = 10$ ). For dielectrics, the CLD prescription had the lowest relative error, followed by FCD and LDR, with the RRC last. For metals, all prescriptions showed a similar behavior. We highlight the fact that this improvement is only due to the formulation of the polarizability and that changing the interaction term in the DDA may also improve the accuracy [10,28], but that this is outside of the scope of this paper.

Metal and dielectric cubes of different effective radii were also simulated (Fig. 4) using the DDA with different prescriptions for the polarizability, again with a fixed number of dipoles per lambda ( $D_{\text{pl}} = 100$ ). This plot clearly shows that for a high number of dipoles per lambda, the difference between the results obtained using different polarizabilities is negligible, since the effect of the self term  $M_i$  goes to zero as the lattice spacing is reduced.

Finally, in Fig. 5, the absorption cross section for gold spheres and cubes were calculated and compared with Mie theory in the case of spheres and between different prescriptions of polarizability for cubes with a fixed number of dipoles per lambda ( $D_{\text{pl}} = 100$ ). The relative error in the absorption was larger at longer wavelengths since the dielectric constant ( $\epsilon$ ) was larger at those wavelengths; therefore, the effective wavelength was smaller and required a smaller discretization. Also for the absorption, at a high enough number of dipoles

per lambda, the difference between different prescriptions of polarizability was negligible.

In general, the case of a dielectric particle was simulated by the DDA much better than that of a metal, as the DDA is limited to simulating materials with a large refractive index. This is because for dielectrics, the variations of the field between the inside and outside of the structure are not as large as in metals, and therefore, the discretization done by the DDA is able to mimic the actual field more precisely. Indeed, the higher accuracy at relatively low  $D_{\text{pl}}$  of the DDA calculations with CLD polarizability that involve dielectrics compared to other formulations of the polarizability for the DDA can be very useful for large simulations (for example, for simulations involving many different scatterers, where one is effectively limited by the computation time in the number of dipoles for each scatterer).

#### 4. SUMMARY

The DDA has been extended to the case of a cuboidal point lattice (DDA with CLD polarizability) with an accurate expression of the polarizability of each cuboidal element. Compared to the DDA using other formulations of the polarizability, such as the FCD, LDR, or RRC, and in the case of dielectrics, this formulation has been shown to have the lowest relative error for a small number of dipoles per lambda. Moreover, the

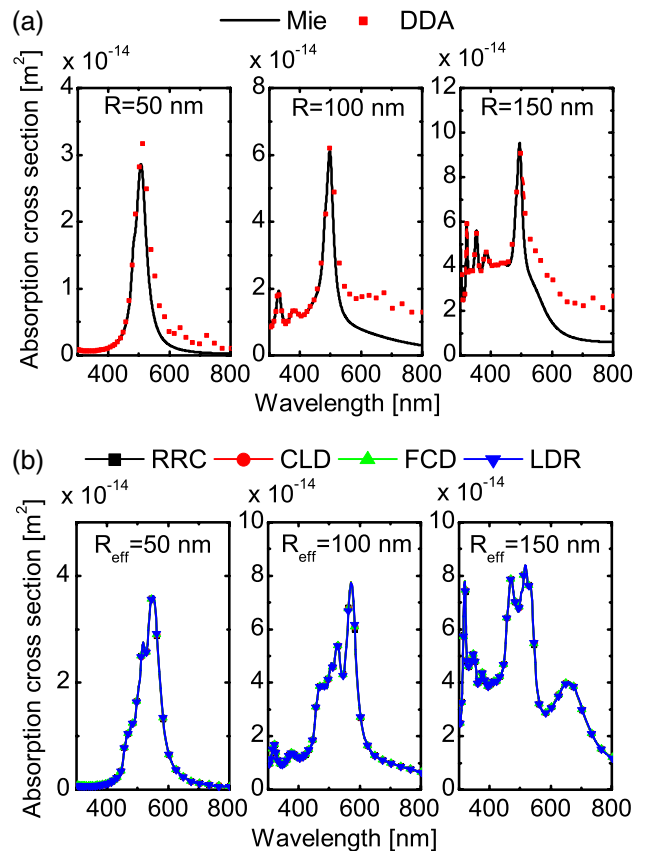


Fig. 5. (a) Comparison between the absorption cross section of gold spheres of different radii ( $R = 50, 100, 150$  nm) calculated using the DDA with CLD polarizability and Mie theory. (b) Comparison between the absorption cross section of gold cubes of different effective radii ( $R_{\text{eff}} = 50, 100, 150$  nm) calculated using different prescriptions of the polarizability. The calculations were done with a fixed number of dipoles per lambda ( $D_{\text{pl}} = 100$ ).

analytical extension to a cuboidal point lattice enables one to overcome the limitation of using a cubic lattice with the same element size, and this may be more suitable for specific simulations, e.g., with elongated geometries or with large field variations. This result enables improvements of simulations in many technologically promising fields such as in optical sensors and in photovoltaic and light emitting devices.

## ACKNOWLEDGMENTS

This work was supported by EPSRC and the Leverhulme Trust.

## REFERENCES

1. B. T. Draine and P. J. Flatau, "Discrete-dipole approximation for scattering calculations," *J. Opt. Soc. Am. A* **11**, 1491–1499 (1994).
2. E. M. Purcell and C. R. Pennypacker, "Scattering and absorption of light by nonspherical dielectric grains," *Astrophys. J.* **186**, 705–714 (1973).
3. B. T. Draine, "The discrete-dipole approximation and its application to interstellar graphite grains," *Astrophys. J.* **333**, 848–872 (1988).
4. M. A. Yurkin and A. G. Hoekstra, "The discrete dipole approximation: an overview and recent developments," *J. Quant. Spectrosc. Radiat. Transfer* **106**, 558–589 (2007).
5. J. J. Goodman, B. T. Draine, and P. J. Flatau, "Application of fast-Fourier-transform techniques to the discrete-dipole approximation," *Opt. Lett.* **16**, 1198–1200 (1991).
6. C. Smith, A. Peterson, and R. Mittra, "A conjugate gradient algorithm for the treatment of multiple incident electromagnetic fields," *IEEE Trans. Antennas Propag.* **37**, 1490–1493 (1989).
7. M. A. Yurkin, "Computational approaches for plasmonics," in *Handbook of Molecular Plasmonics*, F. Della Sala and S. D'Agostino, eds. (Pan Stanford, 2013), pp. 83–135.
8. B. T. Draine and J. J. Goodman, "Beyond Clausius–Mossotti: wave propagation on a polarizable point lattice and the discrete dipole approximation," *Astrophys. J.* **405**, 685–697 (1993).
9. N. B. Piller and O. J. F. Martin, "Increasing the performance of the coupled-dipole approximation: a spectral approach," *IEEE Trans. Antennas Propag.* **46**, 1126–1137 (1998).
10. P. C. Chaumet, A. Sentenac, and A. Rahmani, "Coupled dipole method for scatterers with large permittivity," *Phys. Rev. E* **70**, 036606 (2004).
11. M. A. Yurkin and A. G. Hoekstra, "User manual for the discrete dipole approximation code ADDA 1.2," 2013, [http://a-dda.googlecode.com/svn/tags/rel\\_1.2/doc/manual.pdf](http://a-dda.googlecode.com/svn/tags/rel_1.2/doc/manual.pdf).
12. S. A. Maier, *Plasmonics: Fundamentals and Applications* (Springer, 2007).
13. V. Giannini, A. I. Fernández-Domínguez, S. C. Heck, and S. A. Maier, "Plasmonic nanoantennas: fundamentals and their use in controlling the radiative properties of nanoemitters," *Chem. Rev.* **111**, 3888–3912 (2011).
14. W. L. Barnes, A. Dereux, and T. W. Ebbesen, "Surface plasmon subwavelength optics," *Nature* **424**, 824–830 (2003).
15. V. Giannini, J. A. Sánchez-Gil, O. L. Muskens, and J. G. Rivas, "Electrodynamic calculations of spontaneous emission coupled to metal nanostructures of arbitrary shape: nanoantenna-enhanced fluorescence," *J. Opt. Soc. Am. B* **26**, 1569–1577 (2009).
16. V. Giannini, A. Berrier, S. A. Maier, J. A. Sánchez-Gil, and J. G. Rivas, "Scattering efficiency and near field enhancement of active semiconductor plasmonic antennas at terahertz frequencies," *Opt. Express* **18**, 2797–2807 (2010).
17. D. Gutkovic-Krusin and B. T. Draine, "Propagation of electromagnetic waves on a rectangular lattice of polarizable points," arXiv astro-ph/0403082 (2004).
18. A. Moroz, "Depolarization field of spheroidal particles," *J. Opt. Soc. Am. B* **26**, 517–527 (2009).
19. H.-Y. Xie, M.-Y. Ng, and Y.-C. Chang, "Analytical solutions to light scattering by plasmonic nanoparticles with nearly spherical shape and nonlocal effect," *J. Opt. Soc. Am. A* **27**, 2411–2422 (2010).
20. M. A. Yurkin and M. Kahnert, "Light scattering by a cube: accuracy limits of the discrete dipole approximation and the T-matrix method," *J. Quant. Spectrosc. Radiat. Transfer* **123**, 176–183 (2013).
21. R. A. de la Osa, P. Albella, J. M. Saiz, F. González, and F. Moreno, "Extended discrete dipole approximation and its application to bianisotropic media," *Opt. Express* **18**, 23865–23871 (2010).
22. D. A. Smith and K. L. Stokes, "Discrete dipole approximation for magneto-optical scattering calculations," *Opt. Express* **14**, 5746–5754 (2006).
23. O. J. F. Martin and N. B. Piller, "Electromagnetic scattering in polarizable backgrounds," *Phys. Rev. E* **58**, 3909–3915 (1998).
24. A. D. Yaghjian, "Electric dyadic Green's functions in the source region," *Proc. IEEE* **68**, 248–263 (1980).
25. L. Novotny and B. Hecht, *Principles of Nano-Optics* (Cambridge University, 2012).
26. E. Massa, S. A. Maier, and V. Giannini, "An analytical approach to light scattering from small cubic and rectangular cuboidal nanoantennas," *New J. Phys.* **15**, 063013 (2013).
27. M. A. Yurkin and A. G. Hoekstra, "The discrete-dipole-approximation code ADDA: capabilities and known limitations," *J. Quant. Spectrosc. Radiat. Transfer* **112**, 2234–2247 (2011).
28. M. A. Yurkin, M. Min, and A. G. Hoekstra, "Application of the discrete dipole approximation to very large refractive indices: filtered coupled dipoles revived," *Phys. Rev. E* **82**, 036703 (2010).
29. R. Fuchs, "Theory of the optical properties of ionic crystal cubes," *Phys. Rev. B* **11**, 1732–1740 (1975).